IEICE Communications Express, Vol.13, No.7, 235–239

ComEX

LETTER

Electronically reconfigurable 100-GHz band reflectarray for wireless communication based on microfiber/liquid crystal composite

Trong Nghia Lang[1], **Yo Inoue**[1], **and Hiroshi Moritake**[1, a)]

Abstract This letter introduces an electronically reconfigurable 100-GHz band reflectarray (RA) utilizing a microfiber/liquid crystal composite. The unit cell design is analyzed through full-wave simulations, while experimental measurements elucidate the RA's characteristics, including reflected power, steering range, and switching times. Results demonstrate that the proposed RA exhibits significant continuous beam steering capabilities, ranging from −40° to 40° at 100 GHz, with swift switching times of less than 230 ms. The maximum reflected power achieves −3.5 dB compared to a metal plate of the same size.

Keywords: reflectarray, millimeter wave, liquid crystal, microfiber
Classification: Antennas and propagation

1. Introduction

The relentless growth in the demand for high-capacity, high-speed communication, driven by advancements in wireless technology, is evident. Concurrently, mobile terminals' communication frequency band expands with each new generation. Fifth-generation (5G) communications employ the highest frequency band at approximately 28 GHz for commercial use, poised to extend up to 90 GHz for 5G evolution (5G EVO). Moreover, millimeter waves (MMW) exceeding 90 GHz are gaining attention as a potential frequency band for the next generation (6G) [1]. However, the utilization of higher frequency bands introduces a significant challenge — an increased occurrence of coverage holes due to high straightness. The reflectarray (RA) emerges as an effective method, offering cost and time savings compared to constructing new base stations or adding repeaters. The concept revolves around reflecting radio waves from existing base stations to the coverage holes, providing a technically feasible solution to enhance communication range, rather than relying on directly transmitted waves.

To manipulate the direction of the reflected wave, RAs are often designed with patterns of continuously varying sizes [2] or employ tunable elements such as ferroelectric [3], micro-electromechanical systems (MEMS) [4], and liquid crystal (LC) [5, 6, 7, 8, 9, 10]. RAs using ferroelectrics and MEMS exhibit exceptionally rapid response times, typically on the order of μs. However, there is a scarcity of reports on this topic, and most of their practical applications are confined to the low-frequency MMW range. On the other hand, LC offers a simple structure and allows for continuous adjustment through an external electric field. However, the drawback of LCs lies in their extended decay time, typically ranging from several seconds to several 10 s with a LC layer thickness of several 10 μm, depending on the LC material. In a previous study, we reported a method to accelerate the decay time of a thick LC layer without significantly impacting its inherent dielectric anisotropy, using electrospun-aligned microfiber (MF) [11]. In this letter, we propose a low-cost 100-GHz band RA based on MF/LC composite that can steer the incident plane wave in the desired direction, covering a range over 80° with fast switching times of less than 230 ms.

2. Design of RA's unit cell

Figures 1(a) and (b) depict the analytical model of the unit cell structure conducted using CST Studio Suite with a periodic structure and Floquet port. The unit cell design integrates two single-sided copper-clad laminates (CCL) with the MF/LC layer positioned between them. In this configuration, the upper CCL's copper foil is precisely etched to form electrodes responsible for controlling LC molecules. Conversely, the lower CCL's copper foil serves as a ground without requiring pretreatment. The dielectric board beneath it has no impact on the RA's operation, allowing its exclusion from the analysis model. CCL (Nippon pillar, NPC-F260A) is characterized with $\varepsilon = 2.8$ and $\tan\delta = 0.005$ at 100 GHz, while the copper foil thickness is specified at 9 μm. Addi-

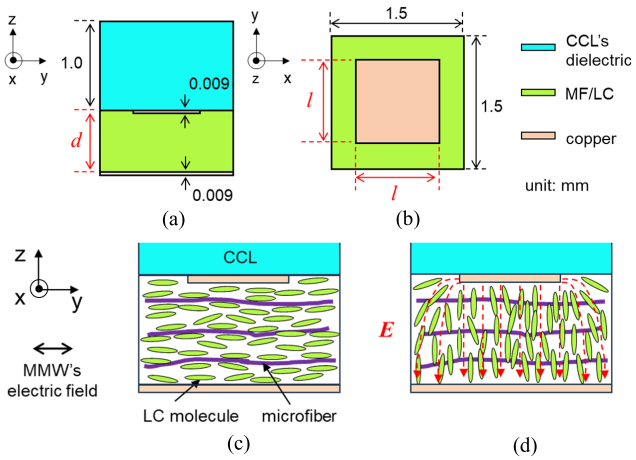

Fig. 1 Simulation model of the RA unit cell (a) side view, (b) top view, and the RA unit cell when (c) no bias is applied, (d) LC molecules are biased

[1] Dept. of Electrical Engineering, National Defense Academy, Yokosuka, Kanazawa 239-0811 Japan
[a)] moritake@nda.ac.jp

DOI: 10.23919/comex.2024XBL0041
Received March 4, 2024
Accepted March 25, 2024
Publicized May 9, 2024
Copyedited July 1, 2024

tionally, a novel nematic LC material (DIC, SL004) is employed, which has $\varepsilon_{min} = 2.5$, $\varepsilon_{max} = 3.3$, and $\tan\delta = 0.01$ in the composite state with MF at 100 GHz. The unit cell period is set at 1.5 mm, and a square patch with a side length l is positioned at the center. Figures 1(c) and (d) illustrate the operational principle of the RA using MF/LC composite. In the non-bias state, LC molecules experience anchoring forces from MFs, aligning themselves along the fiber direction. Upon the application of an external voltage, LC molecules reorient in the direction of the electric field, leading to a change in the MF/LC dielectric constant and the phase of the reflected wave. Notably, LC molecules in the composite exhibit movement within the space between the MF layers (only a few micrometers), significantly reducing the response time compared to LC in its pure state [11].

To identify the optimal unit cell structure for the RA operating at the 100 GHz band, the MF/LC dielectric constant ε is fixed at the central value of 2.9, while the patch's side length l varies in a range of 0.2–1.4 mm. The simulation results in Fig. 2 show that the first resonant frequency varies with the patch length, shifting toward higher frequencies as the patch size decreases. In the case of $d = 1.0$ mm, resonance at near 100 GHz is observed when l approaches 0.69 mm. Conversely, for $d = 0.6$ mm, no resonance occurs in the 100 GHz band despite varying l across the entire range from 0.2 to 1.4 mm. Figure 3 shows the simulated reflection coefficients of the RA using an MF/LC layer thickness of 1.0 mm and a patch length of 0.69 mm, with variations in the MF/LC dielectric constant. Although the dielectric property of MF/LC in the bias state is inhomogeneous as depicted in Fig. 1(d), we focus solely on two cases: when the dielectric constant ε reaches its minimum and maximum values. This approach enables us to simplify analysis and estimate the largest phase change achievable for each RA structure. It is evident that the resonant frequency shifts to the lower frequency side as the MF/LC dielectric constant increases. Consequently, the phase shift follows the same trend, with the phase change at each frequency reaching its maximum value, equal to the difference between the phases at $\varepsilon = 2.5$ and $\varepsilon = 3.3$ (black and blue lines). The aforementioned RA exhibits a maximum loss of about 5.6 dB and a maximum phase change of about 315.1° at 100 GHz. Similar analyses for various MF/LC layer thicknesses are conducted and summarized in Table I.

We observe two significant phase changes: about 300° when the MF/LC layer thickness approaches 50 μm and about 315° at 1 mm. However, the RA using an MF/LC layer thickness of 50 μm (50-μm RA) exhibits higher loss compared to the one with a thickness of 1 mm (1-mm RA). The simulated electric field distributions of the MMW in Fig. 4 reveal that the 1-mm RA has an electric field in the MF/LC layer similar to the incident wave, with the magnitude gradually decreasing toward the copper surface. In contrast, for the 50-μmm RA, the field is directed perpendicular to the incident wave, and the magnitude near the copper surface remains high. These findings align well with the simulation results of the MMW surface current depicted in Fig. 5. In the 50-μm RA, the surface current intensity

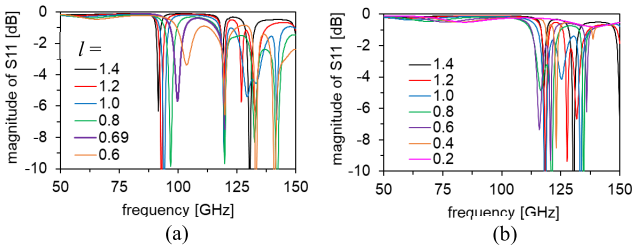

Fig. 2 Reflection coefficients of RAs with various patch lengths l when ε= 2.9 and d= (a) 1.0 mm, (b) 0.6 mm

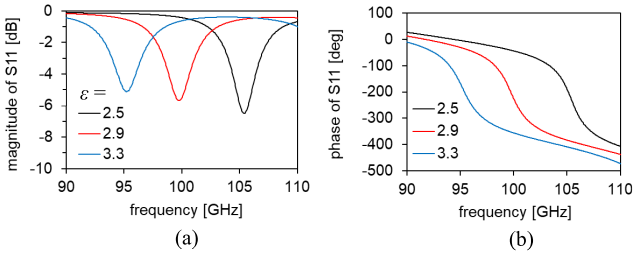

Fig. 3 Reflection coefficients of RA with various MF/LC dielectric constants ε when d= 1.0 mm and l= 0.69 mm (a) magnitude, (b) phase

Table I Simulated results of 100-GHz band RAs with various MF/LC layer thicknesses

Thickness (mm)	Patch length (mm)	Max phase change (deg)	Max loss (dB)
0.025	0.82	21.3	10.1
0.05	0.78	301.1	8.9
0.075	0.74	258.6	4.3
0.1	0.71	215.2	2.8
0.2	0.61	96.9	1.0
0.3	0.46	38.9	0.5
0.4	0.23	31.8	0.4
0.5–0.8	×	×	×
0.9	1.10	19.2	6.4
1.0	0.69	315.1	5.6
1.1	0.56	202.8	1.8
1.2	0.43	128.4	1.1

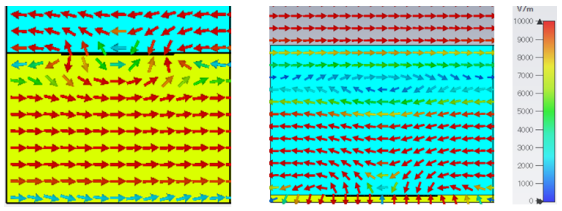

Fig. 4 Simulated results of MMW electric field distribution in the unit cell using MF/LC layer thickness of (a) 1 mm, (b) 50 μm

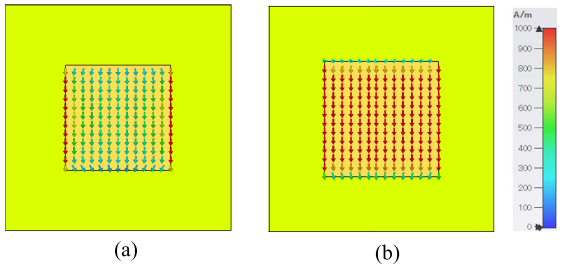

Fig. 5 Simulated results of surface current distribution in the unit cell using MF/LC layer thickness of (a) 1 mm, (b) 50 μm

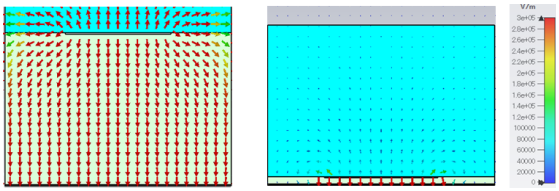

Fig. 6 Simulated results of bias electric field distribution in the unit cell using MF/LC layer thickness of (a) 1 mm, (b) 50 μm

is markedly higher, resulting in larger conductor losses, as illustrated in Table I. Figure 6 shows the simulated results at direct current (DC), in which the bias electric field is distributed over most of the 1-mm RA's structure but is confined to the area below the patch in the 50-μm RA. This implies that only about 25% of the total LC molecules will respond, even when subjected to DC or alternate current (AC) bias, posing a technical challenge in achieving the simulated result of about 300°. Based on the aforementioned results, we choose the 1-mm structure for the practical implementation of the RA, proceed with its fabrication, and conduct a comprehensive evaluation of its characteristics.

3. Measurement setup and results

Figures 7(a) and (b) illustrate the RA design: one CCL serves as the ground (GND) substrate, while another undergoes processing to function as a patch array with 12×12 elements. A 1-mm thick MF layer is sandwiched between them, and finally, the LC is injected. The fluidity of LC molecules facilitates their filling of the spaces between fibers, forming the MF/LC composite naturally and rapidly. Notably, for a structure employing pure LC, a complicated process involving the creation of alignment layers and rubbing is essential. Figures 7(c) and (d) show the magnified image and appearance of the fabricated patch array, respectively. A bias wire is individually designed for each column of the patch array, with a width reduced to 20 μm to ensure minimal impact on the RA properties. The patch array, with an average patch length of 0.686 mm (l = 0.69 mm) and an average wire width of 23.8 μm (w = 20 μm), is successfully manufactured.

A bistatic radar cross section (RCS) measurement setup is prepared to evaluate the reflection properties of the RA, as depicted in Fig. 8. Here, the plane wave is illuminated onto the RA from a transmitting antenna (Tx), and the corresponding reflected wave is captured by the receiving antenna (Rx). The RA's RCS value is assessed through the comparison method, involving measuring the reflected power of a flat copper plate of identical size (20 mm × 20 mm) placed in the same location, serving as a reference. Notably, for a flat plate, the RCS value is equal to $4\pi A^2/\lambda^2$, where A is the area of the plate [12]. Furthermore, spatial constraints exist in front of Tx and adjacent to the enclosure wall, limiting the measurement range to ±10° – ±85°. Figure 9 depicts a monostatic RCS setup with single antenna (Tx/Rx) for measuring the reflected phase and RCS value of the RA. Here, the RA's RCS value is calculated by comparing it to the copper plate's RCS value (approximately −6.5 dBsm).

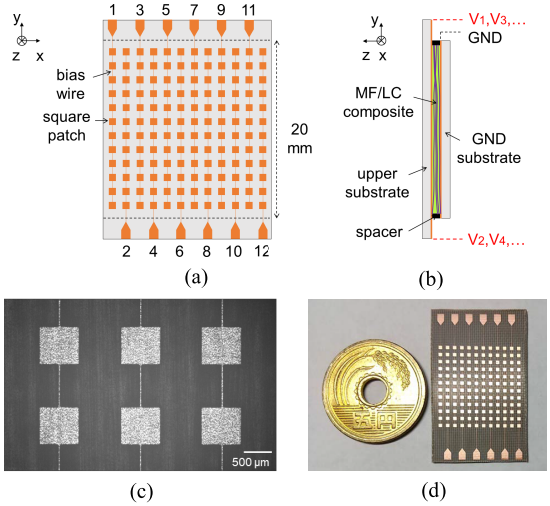

Fig. 7 (a) Top view, (b) side view of the 100-GHz band RA using 1 mm-thick MF/LC layer, and (c) microscope image, (d) appearance of patch array

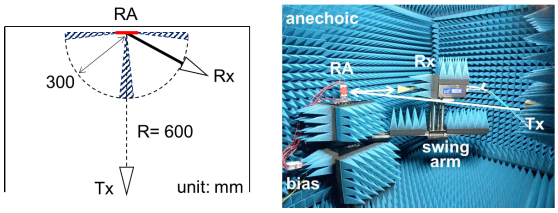

Fig. 8 Measurement setup for the beam pattern of the RA

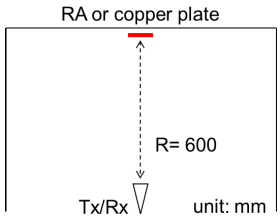

Fig. 9 Measurement setup for the reflected phase and RCS value of the RA in the normal direction

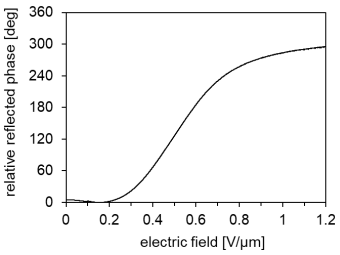

Fig. 10 Experimental relationship between the reflected phase and bias electric field strength under 100 GHz plane wave illumination

Figure 10 shows the trend in the reflected phase change when altering the electric field of the AC bias (sine wave, 1 kHz) across all RA elements, in which the phase difference varies with the electric field strength and reaches 300° at 1.2 V/μm. It is evident that the phase is approaching the saturation value but cannot reach 360° because the maximum attainable value is 315°. Opting for a new LC material with a larger dielectric anisotropy would be a more suitable choice and would contribute to resolving this issue. Figure 11(a)

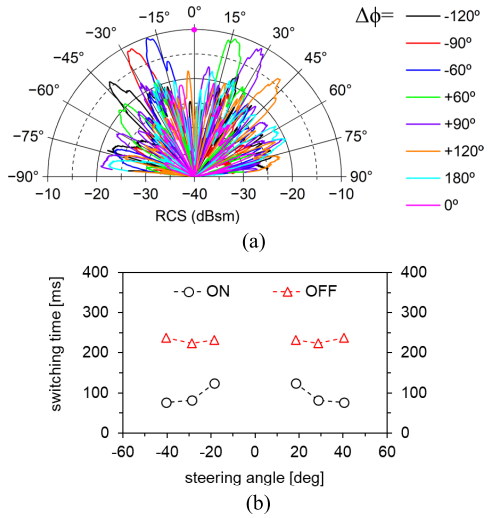

Fig. 11 (a) Various steered beams and (b) switching times of the 100-GHz band RA using 1 mm-thick MF/LC layer

shows the measured RCS patterns for phase differences $\Delta\phi$ between patch columns of 0°, ±60°, ±90°, ±120°, and 180°. Due to the insufficient phase of less than 360°, it was not feasible to set phase differences at ±30° and ±150°. As shown in Fig. 11(a), the RCS values peak at approximately −10 dBsm, with the side lobe level measuring less than −6 dB at all the phase differences. When configuring phase differences of ±60°, ±90°, and ±120°, reflected beams are observed with decreasing magnitudes as the steering angles increase. With the phase difference of 180°, the main beam's reflected power sharply decreases to about −20 dBsm, rendering the device ineffective as a reflector. In this study, we effectively achieved continuous control of the reflected beam over a wide scanning range, spanning from −41.2° to +40.4°.

The switching times of the RA are determined by the magnitude of the signal received by Rx. The switch-on (ON) time, which transitions the beam from the front to a specific direction, is defined as the time it takes for the received magnitude to reach 90% of its maximum. Similarly, the switch-off (OFF) time, which returns the beam from a specific direction to the front, is recorded when the received magnitude falls below 10%. As illustrated in Fig. 11(b), the ON times range from several tens to several hundreds of milliseconds and decrease with increasing steering angles. This observation can be attributed to the accelerated movement of LC molecules in a higher electric field. Conversely, the OFF time remains approximately constant at about 230 ms across all steering angles. Note that the decay time of LC molecules in the pure state is proportional to the square of the LC layer thickness [13]. If pure LC (SL004) with the same thickness of 1 mm is employed, the OFF time would be over 1000 s, indicating the significant enhancement effect of the MFs. Table II presents a comparison of various MMW RAs. The RA proposed in this study demonstrates exceptional characteristics, including a broad steering range of over 80°, a low side lobe level below −6 dB across the entire range, and fast switching times of less than 230 ms. This RA could serve as a simple and efficient solution to coverage holes, and its effectiveness has the potential to be further enhanced through practical improvements.

Table II Comparison of various MMW RAs

Ref.	GHz	Material (thickness)	Total steering range	Max side lobe level	Switching times
[3]	32	ferroelectric	25°	-7 dB	µs
[4]	35.5	MEMS	48°	< -10 dB	µs
[5]	35	LC (127 µm)	40°	-4 dB	N/A
[6]	38	LC (100 µm)	14°	< -10 dB	(several s
[7]	77	LC (50 µm)	40°	-3 dB	to
[8]	77	LC (50 µm)	35°	-5 dB	several
[9]	78	LC (50 µm)	12°	-6 dB	10 s)
[10]	100	LC (75 µm)	55°	< -10 dB	2 s
this work	100	MF/LC (1 mm)	80°	-6 dB	< 230 ms

4. Conclusion

An electronically reconfigurable RA, designed for the 100 GHz band, is fabricated and evaluated using a bistatic RCS system. The model comprises 12 × 12 square patch elements, each with a side length of about 0.7 mm and features a 1-mm thick layer of MF/LC composite as the tunable substrate. Measurement results reveal that the RA exhibits continuous steering capabilities over a broad range spanning from −40° to +40°, with a low side lobe below −6 dB and fast switching times of less than 230 ms. Possessing a straightforward and cost-effective structure, this RA offers a prompt and efficient solution to address the potential issue of coverage holes in future wireless communications.

Acknowledgments

The authors wish to thank DIC Corporation for providing the LC materials. This work was supported by JSPS KAKENHI Grant Number 20K04572.

References

[1] NTT DOCOMO, "5G Evolution and 6G," White Paper, pp. 4–12, January 2023. https://www.docomo.ne. jp/english/ binary/pdf/ corporate/technology/whitepaper_6g/DOCOMO_6G_White_PaperEN_v5.0.pdf

[2] A. Uemura, T. Katoh, T. Arima, and W. Kubo, "Single-layer frequency selective dual-band reflectarray operating at 28 GHz and 39 GHz," *IEICE Commun. Express*, vol. 12, no. 3, pp. 84–89, Dec. 2022. DOI: 10.1587/comex.2022XBL0169

[3] K.K. Karnati, M.E. Trampler, and X. Gong, "A monolithically BST-integrated *Ka*-band beamsteerable reflectarray antenna," *IEEE Trans. Antennas Propag.*, vol. 65, no. 1, pp. 159–166, Jan. 2017. DOI: 10.1109/TAP.2016.2627007

[4] C. Guclu, J. Perruisseau-Carrier, and O. Civi, "Proof of concept of a dual-band circularly-polarized RF MEMS beam-switching reflectarray," *IEEE Trans. Antennas Propag.*, vol. 60, no. 11, pp. 5451–5455, Nov. 2012. DOI: 10.1109/TAP.2012.2207690

[5] A. Moessinger, R. Marin, S. Mueller, J. Freese, and R. Jakoby, "Electronically reconfigurable reflectarrays with nematic liquid crystals," *Electron. Lett.*, vol. 42, no. 16, pp. 899–900, Aug. 2006. DOI: 10.1049/el:20061541

[6] X. Li, H. Sato, Y. Shibata, T. Ishinabe, H. Fujikake, and Q. Chen, "Liquid crystal based reflectarray for reconfigurable intelligent surface applications," *IEICE Commun. Express*, vol. 12, no. 6, pp. 265–270, March 2023. DOI: 10.1587/comex.2023SPL0014

[7] S. Bildik, S. Dieter, C. Fritzsch, M. Frei, C. Fischer, W. Menzel, and R. Jakoby, "Reconfigurable liquid crystal reflectarray with extended tunable phase range," Proc. 41st European Microwave Conf., Manchester, UK, pp. 1292–1295, Oct. 2011. DOI: 10.23919/EuMC.2011.6101792

[8] R. Marin, A. Moessinger, F. Goelden, S. Mueller, and R. Jakoby, "77

GHz reconfigurable reflectarray with nematic liquid crystal," Proc. 2nd European Conf. Antennas and Propagation, Edinburgh, Scotland, pp. 1–5, Nov. 2007. DOI: 10.1049/ic.2007.0940

[9] S. Bildik, S. Dieter, C. Fritzsch, W. Menzel, and R. Jakoby, "Reconfigurable folded reflectarray antenna based upon liquid crystal technology," *IEEE Trans. Antennas Propag*., vol. 63, no. 1, pp. 122–132, Jan. 2015. DOI: 10.1109/TAP.2014.2367491

[10] G. Perez-Palomino, M. Barba, J.A. Encinar, R. Cahill, R. Dickie, P. Baine, and M. Bain, "Design and demonstration of an electronically scanned reflectarray antenna at 100 GHz using multiresonant cells based on liquid crystals," *IEEE Trans. Antennas Propag*., vol. 63, no. 8, pp. 3722–3727, Aug. 2015. DOI: 10.1109/TAP.2015.2434421

[11] T.N. Lang, Y. Inoue, and H. Moritake, "Optimization of the electrospun-aligned microfiber composite with liquid crystal for terahertz wave variable phase shifters," *Jpn. J. Appl. Phys*., vol. 61, no. 7, 071002, July 2022. DOI: 10.35848/1347-4065/ac78ae

[12] L. Sevgi, Z. Rafiq, and I. Majid, "Radar cross section (RCS) measurements [Testing ourselves]," *IEEE Antennas Propag. Mag*., vol. 55, no. 6, pp. 277–291, Dec. 2013. DOI: 10.1109/MAP.2013.6781745

[13] R.A. Soref and M.J. Rafuse, "Electrically controlled birefringence of thin nematic films," *J. Appl. Phys*., vol. 43, no. 5, pp. 2029–2037, May 1972. DOI: 10.1063/1.1661449